Nuclear Engineering and Technology 54 (2022) 1253–1260

Contents lists available at ScienceDirect

Nuclear Engineering and Technology

journal homepage: www.elsevier.com/locate/net

Original Article

Power control of CiADS core with the intensity of the proton beam

Kai Yin [a, b], Wenjing Ma [a], Wenjuan Cui [a], Zhiyong He [a, b, *], Xinxin Li [a, b], Shiwu Dang [a, b], Feng Yang [a, b], Yuhui Guo [a, b], Limin Duan [a, b], Meng Li [a, b], Yikai Hou [a, c]

[a] Institute of Modern Physics, Chinese Academy of Sciences, Lanzhou, 730000, China
[b] School of Nuclear Science and Technology, University of Chinese Academy of Sciences, China
[c] School of Nuclear Science and Technology, Lanzhou University, Lanzhou, 730000, China

ARTICLE INFO

Article history:
Received 15 July 2021
Received in revised form
29 September 2021
Accepted 10 October 2021
Available online 13 October 2021

Keywords:
Accelerator driven system
Core power control
Adjustable aperture
Beam intensity

ABSTRACT

This paper reports the control method for the core power of the China initiative Accelerator Driven System (CiADS) facility. In the CiADS facility, an intense external neutron source provided by a proton accelerator coupled to a spallation target is used to drive a sub-critical reactor. Without any control rod inside the sub-critical reactor, the core power is controlled by adjusting the proton beam intensity. In order to continuously change the beam intensity, an adjustable aperture is considered to be used at the Low Energy Beam Transport (LEBT) line of the accelerator. The aperture size is adjusted based on the Proportional Integral Derivative (PID) controllers, by comparing either the setting beam intensity or the setting core power with the measured value. To evaluate the proposed control method, a CiADS core model is built based on the point reactor kinetics model with six delayed neutron groups. The simulations based on the CiADS core model have indicated that the core power can be controlled stably by adjusting the aperture size. The response time in the adjustment of the core power depends mainly on the adjustment time of the beam intensity.

1. Introduction

In the framework of nuclear waste management, highly radiotoxic minor actinides could be incinerated in an accelerator driven sub-critical (ADS) system, where a sub-critical reactor is driven by an intense external neutron source provided by an accelerator coupled to a spallation target. The ADS systems may be employed to address several missions (e.g. Refs. [1,2]), including transmuting selected isotopes present in nuclear waste to reduce the burden isotopes on geologic repositories; generating electricity and/or process heat; producing fissile materials for subsequent use in critical or sub-critical systems by irradiating fertile elements. Currently, there are active programs in many countries to develop, demonstrate and exploit ADS technology for nuclear waste transmutation and power generation [3]. Driven by the national demand for safe disposal of nuclear waste as well as the potentials for advanced power generation, an ADS program was initiated in 2011 in the Chinese Academy of Sciences under the frame of “Strategic Priority Research Program” [4]. At the end of 2015, with the purpose of building an accelerator-driven transmutation facility, the China initiative Accelerator Driven System (CiADS) was officially approved by the National Development and Reform Commission of the People's Republic of China. The CiADS facility which includes a proton accelerator, a spallation target cooled with Lead–Bismuth Eutectic (LBE) and a sub-critical reactor cooled also with LBE is a small-size experimental facility for demonstrating the ADS concept at 10 MW power level.

As the first ADS facility at several MW power level, many key technologies have to been developed during the construction of the CiADS facility. One of the key technologies is the power control of the sub-critical reactor. It is well-known that the power control of a pressurized water critical reactor is accomplished with the withdrawal and insertion of the control rods. In the CiADS facility, the control rods are not used in the sub-critical reactor. The core power is controlled by adjusting the beam power of the accelerator, where the beam power can be adjusted by changing either the beam intensity or the duty ratio of the proton beam. The control of the core power in the CiADS facility with the method of the duty ratio has

* Corresponding author. Institute of Modern Physics, Chinese Academy of Sciences, Lanzhou, 730000, China.
E-mail address: zyhe@impcas.ac.cn (Z. He).

https://doi.org/10.1016/j.net.2021.10.011

been considered in Ref. [5]. This paper reports the power control of the sub-critical reactor in the CiADS facility with the method of beam intensity. Up to now, few technique for controlling the beam intensity of a high-power proton accelerator is reported in literatures. The approach for adjusting the beam intensity of the proton accelerator in the CiADS facility is studied in Section 2. The basic idea is to block the outer particles of the beam by using an aperture with an adjustable circular size. As the core part of this paper, the control method of the sub-critical core power for the CiADS facility which is based on the adjustment of beam intensity is proposed in Section 3. In order to evaluate the proposed control method, the simulations with a point kinetic model have been performed. The transfer function for the CiADS's sub-critical reactor is described in Section 4 and the simulation results of the power control are reported in Section 5. Finally, the conclusion is given in Section 6.

2. Control for the beam intensity of accelerator

To demonstrate the ADS concept at 10 MW power level, the proton accelerator in the CiADS facility is designed for the energy of 250 MeV and the maximum intensity of 10 mA. As shown in Fig. 1, the proton accelerator consists of an ion source, a Low-Energy Beam Transport (LEBT) section, a Radio-Frequency Quadrupole (RFQ), a Medium-Energy Beam Transport (MEBT) section, a High-Energy Beam Transport (HEBT) section and many Superconducting Cavities (SCs). A proton beam produced in the ion source is brought through the LEBT section to the entrance of the RFQ. Then, the beam is steered by the MEBT section from the RFQ into the SCs. Finally, a coupling section between the accelerator and the target (A-to-T) is used to bring the protons from the HEBT section into the spallation target.

2.1. Adjustable aperture for intensity control

An effective method of intensity control is to use an adjustable collimator or an adjustable aperture to block the outer particles of the beam. Collimators are widely used in the field of accelerators. For example, in Korea Multi-purpose Accelerator Complex (KOMAC), a collimator with a 10 mm aperture is used to reduce dramatically the proton beam intensity and this enables the provision of a suitable flux density proton beam for a radiation effect test [6]. In cancer research and treatment, tele-cobalt machine uses adjustable collimator system to vary the size and shape of the radiation beam for obtaining clinically acceptable flatness, symmetry and penumbra [7]. An aperture with variable diameters is used to decrease the beam current continuously at the Soreq Applied Research Accelerator Facility (SARAF) in Israel [8].

To adjust beam intensity in the CiADS facility, a circular aperture with variable diameters will be used in the LEBT section. The aperture contains two cylindrical rotating cores which are mirror symmetric to each other. Each cylindrical core is a cylinder with a series of half-moon shaped grooves [9]. When the cylinder rotates from the azimuth angle from 0° to 190°, the diameter of the half-moon groove increases from 0 mm to 40 mm continuously.

One of the developed adjustable apertures has been used in the demonstration accelerator of the CiADS facility. The demonstration accelerator consists of an ion source, an LEBT section, a RFQ, an MEBT section, a SC section and an HEBT section [10]. Fig. 2 shows the ion source and the LEBT section in the demonstration accelerator, where the adjustable aperture has been installed at the LEBT section. The detailed description about the components in the ion source and the LEBT section can be found in Refs. [10,11]. Because of low energy, water cooling is used during the operation of the accelerator. The 4 red water pipes for the aperture device in Fig. 2 are used for the inlet and the outlet of cooling water. The demonstration accelerator of the CiADS facility has been commissioned successfully using Continuous-Wave (CW) and pulsed proton beams. In February 2021, the CW proton beam with the energy of 20 MeV and the beam current of 10 mA has been obtained. The adjustable aperture has been used to control the beam intensity during the operation of the demonstration accelerator.

2.2. Variation of beam intensity with aperture size

The experimental measurements have indicated that the beam intensity increases with the size of the adjustable aperture [9]. In order to observe the variation of beam intensity with both the size of beam spot and the aperture size, the beam intensity is calculated when the diameter of the aperture is changed from 0 mm to 40 mm. In the calculation, the proton beam is assumed to be a Gaussian distribution with an FWHM (Full Width at Half Maximum) of 6, 8, 10 or 12 mm before passing through the aperture. Afterward, the proton beam passes through vertically the aperture, where the center of the beam passes through the center of the aperture.

Fig. 3 shows the relative beam intensity as a function of the rotational angle of the cylinder, where the relative beam intensity is defined as the ratio of the passing protons to the total protons. The results with 4 values of FWHM are compared in the figure. It is shown clearly that the relative beam intensity increases with the rotational angle. On the other hand, at a given rotational angle, the relative beam intensity decreases with the increasing FWHM value. The beam intensity depends on both the rotational angle and the spot size of proton beam.

2.3. Adjustment of beam intensity

In order to automatically adjust the beam intensity, a Proportional Integral Derivative (PID) controller is used by comparing the measured intensity with the setting value. The block diagram of the control system for the beam intensity has been shown in Fig. 1. The

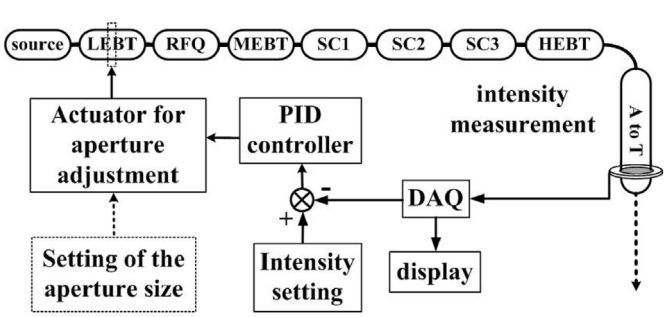

Fig. 1. Block diagram of control system for beam intensity.

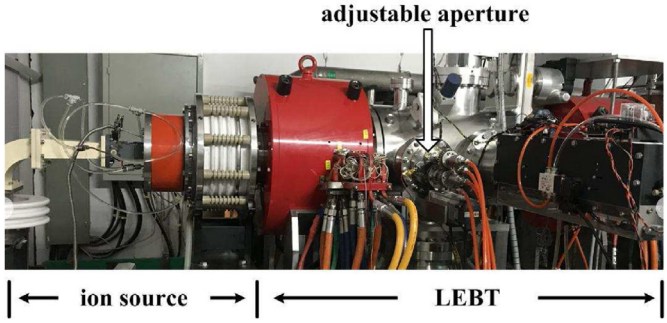

Fig. 2. The adjustable aperture installed at the LEBT section.

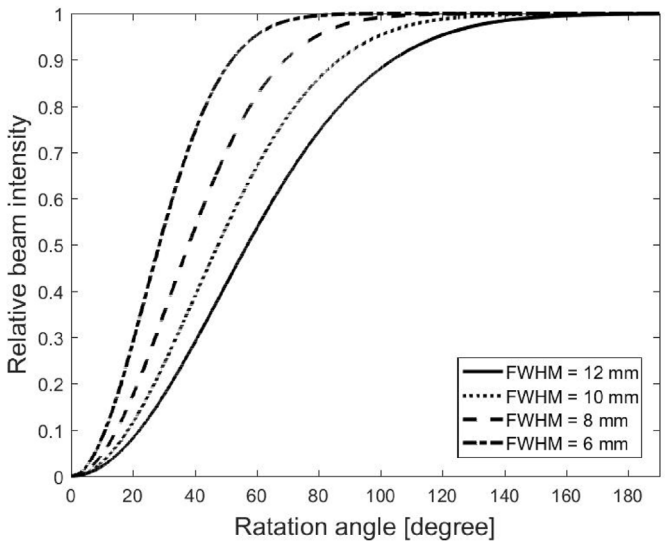

Fig. 3. Relative beam intensity as a function of the rotational angle of the cylinder in the aperture device.

control system of beam intensity includes three main functions, i.e. the measurement of beam intensity, the PID controller and the adjustment of the rotational angle in the aperture device. The measurement of beam intensity is accomplished with a set of beam instrumentation. In the CiADS facility, 9 sets of AC Current-Transformers (ACCTs) and 3 sets of DC Current-Transformers (DCCTs) will be used to measure the beam intensity. The signal measured by the ACCT detector installed at the upstream of the target in the HEBT section will be sent to the control system for the beam intensity, as shown in Fig. 1.

The dynamics of accelerator is not considered in the calculation results in Fig. 3. In fact, when the aperture size is increased, the spot size of proton beam may be increased dramatically. To avoid the beam loss along to the beam line, some devices such as solenoids have to be adjusted manually. Thus, a function for setting manually the aperture size is designed in Fig. 1. The operational modes are described as follows: the beam intensity can be decreased automatically based on the PID controller, while the beam intensity should be increased manually by setting the aperture size.

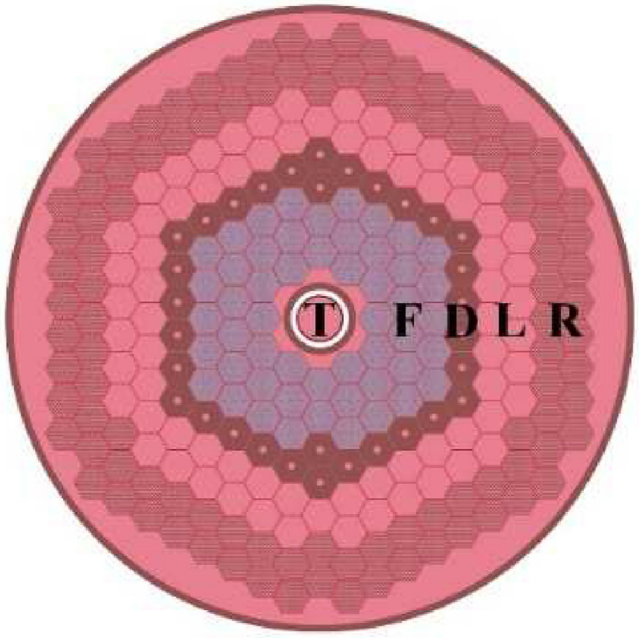

Fig. 4. The layout of the sub-critical reactor core used in OpenMC. "T" denotes the target; "F" denotes the fuel assemblies; "D" denotes the dummy components; "L" denotes the LBE coolants; "R" denotes the reflector region.

3. Control for CiADS core power

In the CiADS facility, the intense external neutron source produced by proton beam bombarding the spallation target located vertically at the centre of the reactor is used to drive the sub-critical core. According to the design of CiADS facility, the control rods are not used in the reactor. The power of the sub-critical core is controlled by changing the proton power, where the proton power is adjusted by either the beam intensity or the duty ratio of the proton beam.

3.1. The sub-critical core in CiADS

The sub-critical reactor in the CiADS facility is a small-size (10 MW) pool-type reactor cooled with LBE. The sub-critical core is composed by wrapped hexagonal Fuel Assemblies (FAs) with pins arranged on a triangular lattice. The active zone is surrounded by dummy elements serving as the reflector. All the primary components are contained in the main reactor vessel with a diameter of 3445 mm.

To calculate the neutronic parameters of the sub-critical core, the simulation is performed with FLUKA [12] and OpenMC codes [13] by considering the proton beam with the energy of 250 MeV and the current of 10 mA bombarding a LBE spallation target located in the center of the sub-critical reactor. The simulation with the FLUKA code is the first step, namely the physical process of proton beam bombarding spallation target; while the simulation with the OpenMC code is the second step, namely the neutron transport process in subcritical reactor coupling with a spallation neutron source.

In the simulation, the proton beam with a Gaussian distribution bombards vertically the target. The cylindrical target container is made of T91 stainless steel and filled with LBE. Its height, inner diameter and outer diameter are 2605 mm, 240 mm and 260 mm, respectively. The sub-critical reactor core with a height of 1000 mm is composed by 52 wrapped hexagonal FAs, where each FA is made of 162 fuel pins arranged on a triangular lattice. Each fuel pin is filled by Uranium dioxide enriched with 19.75% of U_{235}. The layout of the sub-critical reactor core for the CiADS facility used in OpenMC is shown in Fig. 4.

The calculation results about the neutronic parameters in the CiADS core are listed in Table 1. $P(0)$, ρ_0, β and Λ denote the reactor core power, the total reactivity, the total delayed neutron fraction, the neutron generation time, respectively, where $\rho_0 = (k_{eff} - 1)/k_{eff}$. λ_i and β_i with $i = 1, \ldots, 6$ represent the decay constant and the delayed neutron fraction, respectively. The main parameter values of the CiADS core in Table 1 will be used in the simulation with the point kinetic equations for a sub-critical core in Section 5. With $K_{\text{eff}} = 0.96$, the CiADS sub-critical core is a lightly sub-critical reactor. Thus, the point kinetic equations for the lightly sub-critical core in Refs. [14,15] can be used in the following simulation for the CiADS facility.

3.2. Control scheme for core power

The block diagram of the control system for the core power is shown in Fig. 5. As same as that in a pressurized water reactor, the

Table 1
The parameters values of CiADS core.

parameter	value	parameter	value
$P(0)$	10 MW	β_5	1.32e-3
ρ_0	−0.0417	β_6	5.49e-4
Λ	1.5788e-6 s	λ_1	0.0134 s^{-1}
k_{eff}	0.96	λ_2	0.0326 s^{-1}
β	7.50e-3	λ_3	0.1212 s^{-1}
β_1	2.32e-4	λ_4	0.3067 s^{-1}
β_2	1.26e-3	λ_5	0.8649 s^{-1}
β_3	1.23e-3	λ_6	2.9050 s^{-1}
β_4	2.90e-3		

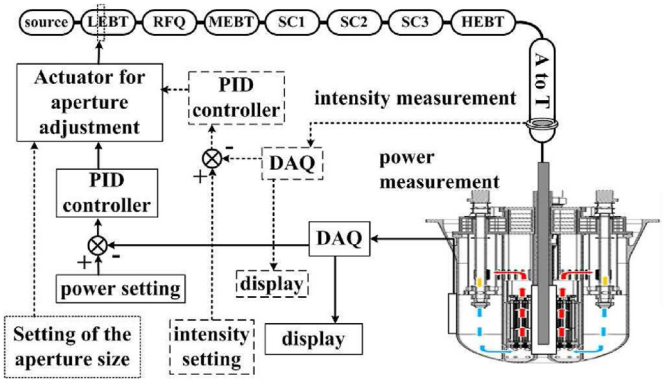

Fig. 5. Block diagram of control system for core power.

system of excore nuclear instrumentation is used to provide indication of reactor power during the operations of CiADS facility. Three operational modes which denote intensity, power and aperture modes exist in the control system in Fig. 5. In the intensity mode, as described in sub-section 2.3, the measure value of the beam intensity is compared with the setting value. Then, the PID controller based on the comparison results of the beam intensity is used to adjust the rotational angle of the aperture. In the power mode, the PID controller based on the comparison results of the reactor power is used to adjust the rotational angle of the aperture. Both the intensity and power modes are the automatic control modes.

By considering the uncertainty or variation of the beam intensity during the operation in the control of the reactor power, the aperture mode which is a manual mode for setting manually the aperture size is designed in Fig. 5. In the aperture mode, the manually setting value of the aperture size is used to adjust the rotational angle in the aperture device. By changing manually the aperture size and the parameters of other devices along the beam line, the power of the reactor core can be adjusted to the setting value. Usually, the automatic power mode is used when the core power has to been decreased, while the manual aperture mode is used when the core power has to been increased.

4. Simulation model for the power control

In order to evaluate whether the control scheme of the CiADS core power shown in Fig. 5 functions well, the simulation is performed with a CiADS core model, where the transfer function of the reactor core based on the point reactor kinetics model is used. The point reactor kinetics model is based on the neutron diffusion model, where the diffusion model is one-step simpler of the Boltzmann transport equation.

The simplified neutronics description in the point kinetic model has proved suitable for a wide range of reactor simulations. For example, for the sub-critical reactor with an external neutron source, the point reactor kinetic model has been used in Ref. [14] to assess the kinetic and dynamic transient behavior of sub-critical reactor in the ADS system. The dynamic behavior of the Italian LBE-cooled ADS system has been studied with the point kinetic model in Ref. [15]. In addition, the core power control of the CiADS facility has also been studied with the point kinetic model [5]. The point kinetic equations in a sub-critical core can be written as follows.

$$\frac{dP(t)}{dt}=\frac{\rho_0+\rho(t)-\beta}{\Lambda}P(t)+\sum_{i=1}^{6}\lambda_i C_i'(t)+Q'(t) \tag{1}$$

$$\frac{dC_i'(t)}{dt}=\frac{\beta_i}{\Lambda}P(t)-\lambda_i C_i'(t),\ \text{with } i=1,\ldots,6 \tag{2}$$

with $C_i'(t)=F\Sigma_f V\upsilon C_i(t)$ and $Q'(t)=F\Sigma_f V\upsilon Q(t)$, where F is the conversion from fission rate to power; Σ_f , V and υ are the macroscopic fission cross section, the reactor volume, and the neutron velocity, respectively. $P(t)$, $C_i(t)$ and $Q(t)$ are the reactor core power, the delayed neutron precursor concentration and the intensity of external neutron source at time t, respectively. $\rho(t)$ is the time-dependent reactivity. Considering $dC_i'(0)/\mathrm{dt}=0$ at time $t=0$ s, (2) can be written as:

$$C_i'(0)=\frac{\beta_i}{\lambda_i\Lambda}P(0) \tag{3}$$

By dividing (1) with $P(0)$ and (2) with$C_i'(0)$, the point kinetic normalized equations can be written as:

$$\frac{dP_r}{dt}=\frac{\rho_0+\rho(t)-\beta}{\Lambda}P_r+\sum_{i=1}^{6}\frac{\beta_i}{\Lambda}C_{ir}+\frac{Q'(0)}{P(0)}Q_r \tag{4}$$

$$\frac{dC_{ir}}{dt}=\lambda_i P_r-\lambda_i C_{ir} \tag{5}$$

with $P_r\equiv P(t)/P(0)$, $C_{ir}\equiv C_i(t)/C_i(0)$and $Q_r\equiv Q(t)/Q(0)$. During the operation of the CiADS facility, the temperature-dependent feedback effects in reactivity need to be considered. The heat transfer equations below which describe the single node transient behavior of temperatures in the fuel and coolants are derived from the energy conservation for the fuel and coolants in the core region, respectively.

$$M_f C_{pf}\frac{dT_f}{dt}=P(t)-U\left(T_f-T_{cavg}\right) \tag{9}$$

$$M_c C_{pc}\frac{dT_{cavg}}{dt}=U\left(T_f-T_{cavg}\right)-WC_{pc}(T_{cout}-T_{cin}) \tag{10}$$

with

$$T_{cavg}=\frac{T_{cout}-T_{cin}}{2} \tag{11}$$

where T_f, T_{cavg}, T_{cout} and T_{cin} denote the fuel averaged temperature, the averaged coolant temperature, the outlet and inlet coolant temperatures, respectively. M_f and M_c are the fuel mass and coolant mass; C_{pf} and $C_{pc}$are specific heat capacity of fuel and coolant, respectively. W is coolant mass flow rate and U is total heat transfer coefficient from fuel to coolant. Then, the time-dependent feedback effects in reactivity due to the changes in the temperatures can be

calculated as follows.

$$\rho(t) = \alpha_f\left(T_f - T_f(0)\right) + \alpha_c\left(T_{cavg} - T_{cavg}(0)\right) + \rho_{per}(t) \tag{12}$$

where, $\rho_{per}(t)$ is reactivity perturbation; α_f and α_c are the fuel and coolant reactivity coefficients, respectively. The thermo-hydraulic parameters used for the simulation of the CiADS reactor core are listed in Table 2 [16].

In order to analyze the features of the proposed controller, the linear model of the CiADS core is derived from the nonlinear equations (4), (5), (9) and (10), by employing first-order perturbation theory and ignoring high-order terms. The linear model which describes the neutronic and thermo-hydraulic behaviors of the CiADS core is expressed as follows:

$$\begin{cases} \dfrac{d\delta P_r}{dt} = \dfrac{\rho_0-\beta}{\Lambda}\delta P_r + \dfrac{\alpha_f}{\Lambda}\delta T_f + \dfrac{\alpha_c}{\Lambda}\delta T_{cavg} + \dfrac{1}{\Lambda}\delta\rho_{per} + \sum_{i=1}^{6}\dfrac{\beta_i}{\Lambda}\delta C_{ir} + \dfrac{Q'(0)}{P(0)}\delta Q_r \\ \dfrac{d\delta C_{ir}}{dt} = \lambda_i\delta P_r - \lambda_i\delta C_{ir}, i = 1,2,3,4,5,6 \\ \dfrac{\mathrm{d}\delta T_f}{\mathrm{d}t} = \dfrac{P(0)\delta P_r}{M_f C_{pf}} - \dfrac{U}{M_f C_{pf}}\left(\delta T_f - \delta T_{cavg}\right) \\ \dfrac{d\delta T_{cavg}}{dt} = \dfrac{U}{M_c C_{pc}}\delta T_f - \dfrac{U+2WC_{pc}}{M_c C_{pc}}\delta T_{cavg} + \dfrac{2WC_{pc}}{M_c C_{pc}}\delta T_{cin} \end{cases} \tag{13}$$

The symbol δ indicates the deviation of a variable from initial steady state value. The linear model in (13) is a model with double inputs and four output, where $\delta\rho_{per}$ and δQ_r are the inputs and δP_r, δT_f, δT_{cavg} and $\rho(t)$ are the outputs. Then, the state space equation of the linear core model is obtained from (13) as follows.

$$\begin{cases} \dot{\boldsymbol{x}}(t) = Ax(t) + Bu(t) \\ y(t) = Cx(t) + Du(t) \end{cases} \tag{14}$$

where

$$\boldsymbol{u}(t) = \left[\delta\rho_{per},\ \delta Q_r\right]^T$$

$$\boldsymbol{y}(t) = \left[\delta P_r, \delta T_f, \delta T_{cavg}, \rho(t)\right]$$

$$\boldsymbol{x}(t) = \left[\delta P_r, \delta C_{r1}, \delta C_{r2}, \delta C_{r3}, \delta C_{r4}, \delta C_{r5}, \delta C_{r6}, \delta T_f, \delta T_{cavg}, \delta T_{cin}\right]^T$$

Table 2
The thermo-hydraulic parameters for the CiADS core.

parameter	Value	parameter	value
M_f	3880 kg	α_f	−1.09e-5
M_c	20200 kg	α_c	−5.9e-6
$T_f(0)$	682.25 k	C_{pf}	303.62 J/(kg*k)
$T_{cavg}(0)$	603.25 k	C_{pc}	146.5 J/(kg*k)
W	541 kg/s		

$$a_1 = \frac{\rho_0-\beta}{\Lambda},\ a_2 = \frac{\alpha_f}{\Lambda},\ ,\ a_3 = \frac{\alpha_c}{\Lambda},\ a_4 = \frac{P(0)}{M_f C_{pf}},\ a_5 = -\frac{U}{M_f C_{pf}},\ a_6 = \frac{U}{M_f C_{pf}},\ a_7 = \frac{U}{M_c C_{pc}},\ a_8 = -\frac{U+2WC_{pc}}{M_c C_{pc}},\ a_9 = \frac{2WC_{pc}}{M_c C_{pc}}$$

$$\boldsymbol{B} = \begin{bmatrix} \frac{1}{\Lambda} & 0 & 0 & 0 & 0 & 0 & 0 & 0 & 0 & 0 \\ \frac{Q'(0)}{P(0)} & 0 & 0 & 0 & 0 & 0 & 0 & 0 & 0 & 0 \end{bmatrix}^T$$

$$\boldsymbol{A} = \begin{bmatrix} a_1 & \frac{\beta_1}{\Lambda} & \frac{\beta_2}{\Lambda} & \frac{\beta_3}{\Lambda} & \frac{\beta_4}{\Lambda} & \frac{\beta_5}{\Lambda} & \frac{\beta_6}{\Lambda} & a_2 & a_3 & 0 \\ \lambda_1 & -\lambda_1 & 0 & 0 & 0 & 0 & 0 & 0 & 0 & 0 \\ \lambda_2 & 0 & -\lambda_2 & 0 & 0 & 0 & 0 & 0 & 0 & 0 \\ \lambda_3 & 0 & 0 & -\lambda_3 & 0 & 0 & 0 & 0 & 0 & 0 \\ \lambda_4 & 0 & 0 & 0 & -\lambda_4 & 0 & 0 & 0 & 0 & 0 \\ \lambda_5 & 0 & 0 & 0 & 0 & -\lambda_5 & 0 & 0 & 0 & 0 \\ \lambda_6 & 0 & 0 & 0 & 0 & 0 & -\lambda_6 & 0 & 0 & 0 \\ a_4 & 0 & 0 & 0 & 0 & 0 & 0 & a_5 & a_6 & 0 \\ 0 & 0 & 0 & 0 & 0 & 0 & 0 & a_7 & a_8 & a_9 \\ 0 & 0 & 0 & 0 & 0 & 0 & 0 & 0 & 0 & 0 \end{bmatrix}$$

$$\boldsymbol{C} = \begin{bmatrix} 1 & 0 & 0 & 0 & 0 & 0 & 0 & 0 & 0 & 0 \\ 0 & 0 & 0 & 0 & 0 & 0 & 0 & 1 & 0 & 0 \\ 0 & 0 & 0 & 0 & 0 & 0 & 0 & 0 & 1 & 0 \\ 0 & 0 & 0 & 0 & 0 & 0 & 0 & \alpha_f & \alpha_c & 0 \end{bmatrix}$$

$$\boldsymbol{D} = \begin{bmatrix} 0 & 0 & 0 & 0 \\ 0 & 0 & 0 & 1 \end{bmatrix}^T$$

Finally, the transfer function of the reactor core is obtained as follows.

$$\boldsymbol{G}(s) = \boldsymbol{C}[s\boldsymbol{I} - \boldsymbol{A}]^{-1}\boldsymbol{B} + \boldsymbol{D} \tag{15}$$

with

$$\boldsymbol{G}(s) = \begin{bmatrix} G_{11}(s) & G_{12}(s) \\ G_{21}(s) & G_{22}(s) \\ G_{31}(s) & G_{32}(s) \\ G_{41}(s) & G_{42}(s) \end{bmatrix} \tag{16}$$

5. The simulation results and discussions

The simulations are performed with the core model discussed in Section 4. Fig. 6 shows the block diagram of the simulation for the control method of the CiADS core power. The input in the simulation is a setting value of the relative power, and the outputs are the simulated values of the relative power, fuel average temperature, coolant average temperature and reactivity, where the relative power is defined as the ratio of the adjusted power to the original power. For example, if the original power and the adjusted power are 10 and 9.6 MW, respectively, the relative power is 0.96.

The block entitled as “PID controller” in Fig. 6 performs the

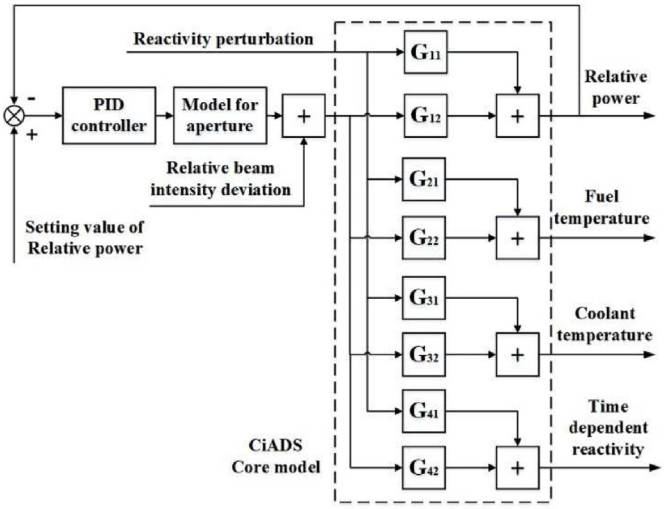

Fig. 6. Block diagram for simulating the power control of the CiADS core.

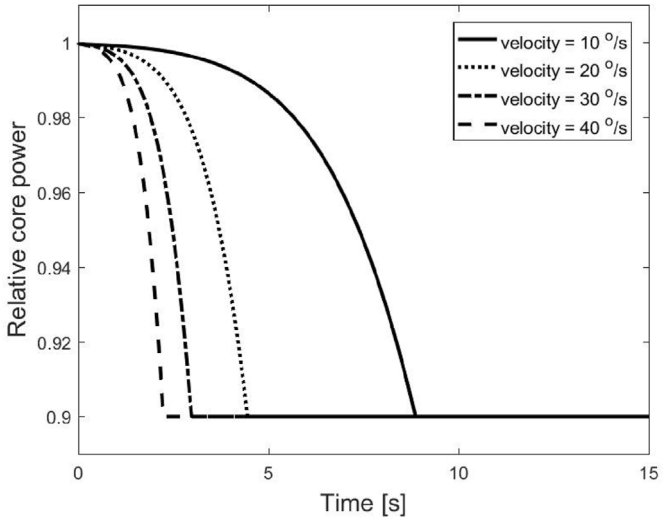

Fig. 7. Relative core power as a function of time. The velocities of 10, 20, 30 or 40°/s are considered for the rotational angle of the aperture.

feedback control action of the relative power. The difference between the simulated value and the setting value of the relative power is sent to the PID controller. By using a proportional coefficient K_p, an integral coefficient K_i and a derivative coefficient K_d, the PID controller calculates the rotational angle $u(t)$ of the aperture device. After receiving the rotational angle $u(t)$ from the PID controller, the block entitled as "Model for aperture" performs the calculation of the new beam intensity as described in sub-section 2.2. As shown in Fig. 3, the beam intensity is a function of both the FWHM of the beam and the rotational angle of the aperture device. The new beam intensity is calculated with a given value of FWHM and the rotational angle $u(t)$ from the PID controller.

The block entitled as "CiADS core model" represents the point kinetic model, where the transfer function G of the reactor core is given in (16). The two inputs of the CiADS core model are the reactivity deviation for G_{11}, G_{21}, G_{31}, G_{41} and the variation in the external neutron source strength for G_{12}, G_{22}, G_{32}, G_{42}. Because the control rods are not used in the core of the CiADS facility, the reactivity deviation is not considered in the following simulation. The simulation focuses mainly on the effect of the external neutron source strength on the relative power, the fuel temperature and the coolant average temperature, where the external neutron source strength is variable by adjusting the beam intensity of proton beam.

5.1. The power control

It has been reported in Ref. [14] that the power of a sub-critical core is directly proportional to the external neutron source strength. In the CiADS facility, with a given beam energy, the strength of spallation neutrons is directly proportional to the beam intensity of proton beam. As discussed in sub-section 2.1, the beam intensity can be adjusted by rotating the angle of the cylinder in the aperture device. Thus, the simulation results for validating the automatic control of the sub-critical core power by adjusting the angle of the aperture device are reported in this sub-section.

The simulation has been performed according to the simulation model in Fig. 6, by considering the effects of two parameters on the relative core power, i.e. the rotational velocity of the cylinder and the spot size of proton beam. The temporal variation of the relative power is shown in Fig. 7, where the results with 4 rotational velocities are compared. The proton beam with an FWHM of 12 mm is used in the simulation, and the setting value of the relative core power is 0.9. At the beginning, the relative core power decreases dramatically with time, and several seconds later, it is stabilized at the setting value of the relative power. The decreasing time changes with the rotational velocity. The falling speed in the temporal variation of the relative power becomes slower as the rotational velocity decreases. The response time in the adjustment of the core power depends mainly on the adjustment time of the aperture.

It is shown clearly that the core power can be controlled automatically by adjusting the beam intensity, where the beam intensity is controlled by changing the rotational angle of the cylinder in the aperture. To achieve a given rotational angle, the time needed for adjusting the rotational angle or the beam intensity is inversely proportional to the rotational velocity. Thus, the time needed for adjusting the relative power varies with the rotational velocity, as shown as in Fig. 7.

Fig. 8 shows the temporal variation of the relative core power when the proton beam with an FWHM of 12, 10, 8 or 6 mm passes through the aperture. The cylinder of the aperture rotates with a fixed velocity of 20°/s, and the setting value of the relative core power is 0.9. As shown as in Fig. 3, at a given rotational angle, the

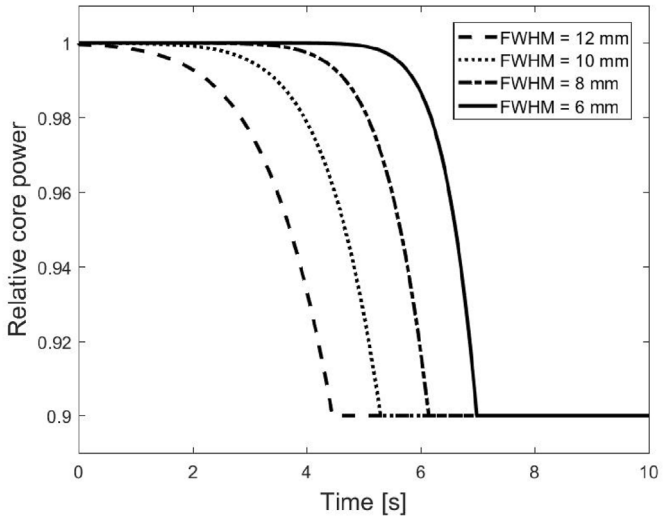

Fig. 8. Relative core power as a function of time. The beams with an FWHM of 12, 10, 8 or 6 mm are compared.

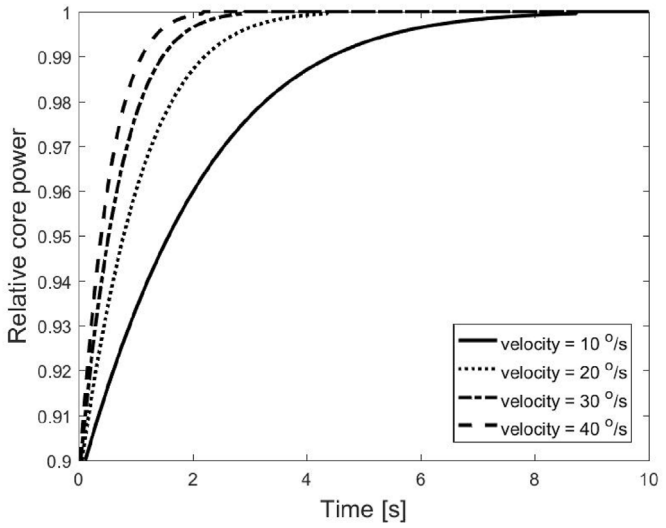

Fig. 9. Relative core power as a function of time. The velocities of 10, 20, 30 or 40°/s are considered for the rotational angle of the cylinder.

beam intensity decreases with the increasing FWHM. Thus, at a given time or a given rotational angle, the relative core power in Fig. 8 also decreases with the increasing FWHM. It is shown in Fig. 8 that the response time in the adjustment of the core power varies with the spot size of proton beam, i.e. the FWHM of proton beam.

The increase of the relative core power with time is shown in Fig. 9, where the cylinder in the aperture device rotates with a velocity of 10, 20, 30 or 40°/s, respectively. The proton beam with an FWHM of 12 mm is used in the simulation, and the relative core power stays at 0.9 before increasing the core power. As same as in Fig. 7, the time for adjusting the core power increases with the decreasing velocity.

Fig. 10 shows the temporal variation of the relative core power when the proton beam with an FWHM of 6, 8, 10 or 12 mm passes through the aperture. The cylinder rotates with a fixed velocity of 20°/s. In the simulation, the relative core power is taken as 1 when the diameter in the aperture attains the maximum value, i.e. 40 mm. At the beginning, the relative core power stays at 0.9. As shown in Fig. 10, the time for increasing the core power varies with the spot size of proton beam.

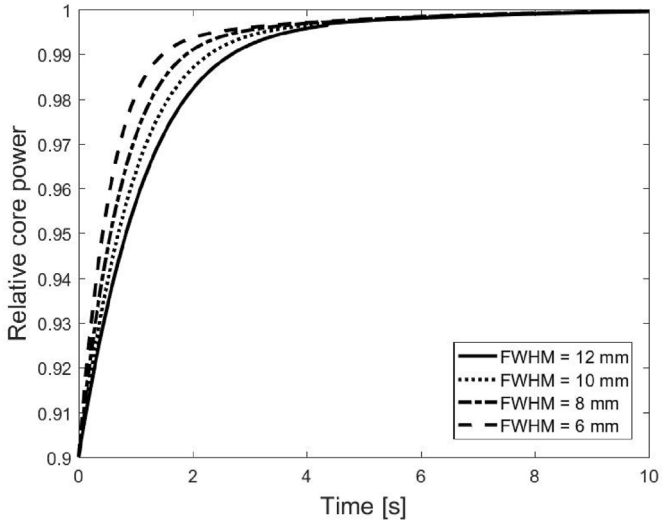

Fig. 10. Relative core power as a function of time. The beams with an FWHM of 12, 10, 8 or 6 mm are compared.

The results from Figs. 7–10 can be briefly summarized as follows. (1) When the beam intensity is adjusted by rotating the cylinder in the aperture, the core power of the CiADS facility depends on both the rotational angle of the cylinder and the spot size of proton beam. Because there is no one-to-one relation between the core power and the rotational angle, it is impossible to give a single calibration between the two physical quantities. (2) Since the core power is measured during the operation of the CiADS facility, the core power can be decreased automatically based on a PID controller by comparing the measured core power with the setting value. (3) To increase the core power, it is suggested to increase manually the circular size of the aperture device because of the following consideration. As discussed in Section 2, when the circular size of the aperture device is increased, the spot size of proton beam is increased dramatically. To avoid the beam loss along to the beam line, other devices in the accelerator have to be adjusted manually.

5.2. The temperature-dependent feedback effect

In this sub-section, the temporal variations of the fuel average temperatures and the coolant average temperatures are analyzed. The temporal variations of the fuel average temperature and the coolant average temperature are shown in Figs. 11 and 12 when the relative core power decreases from 1 to 0.9. The simulation parameters are exactly the same as that in Fig. 7. Because the relative core power decreases, both the fuel average temperature and the coolant average temperature decrease with time for a long period of more than 100 s. As same as that of the core power, the response time of both the fuel average temperature and the coolant average temperature vary with the rotational velocity of the cylinder in the aperture.

Finally, the effect of temperature variations on the core power control is not significant. At time t > 10 s, although the temperatures from Figs. 11 to 12 decreases with time, the relative core powers in Fig. 7 keep unchanged. This is because the core power is adjusted automatically by changing the beam intensity. As listed in (4), the core power depends on both the reactivity and the beam intensity. The effect of reactivity feedback is removed by automatically adjusting the beam intensity.

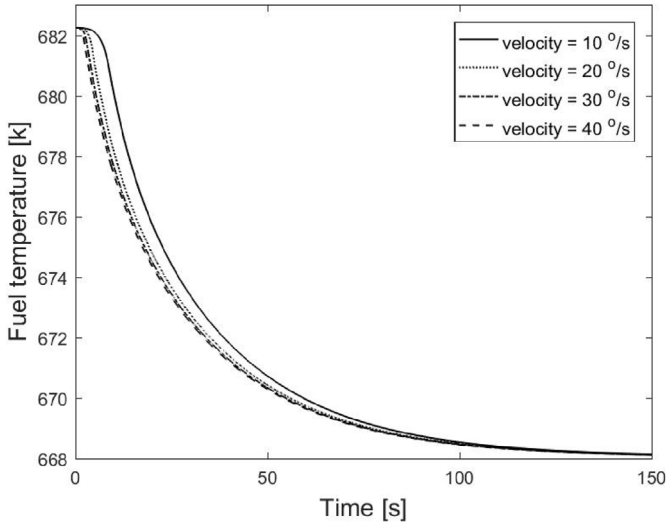

Fig. 11. Temporal variation of fuel temperature when the relative core power decreases from 1 to 0.9.

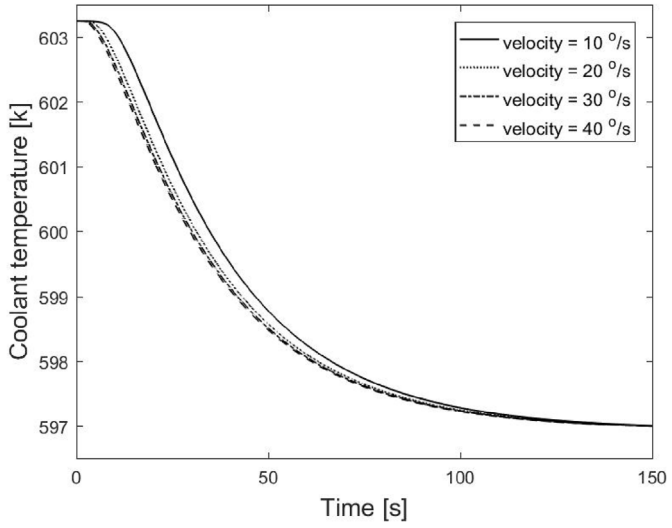

Fig. 12. Temporal variation of coolant average temperature when the relative core power decreases from 1 to 0.9.

6. Summary

The control method for the reactor core power by adjusting the proton beam intensity has been proposed for the CiADS facility. In the proposed control method, the beam intensity is changed by blocking the outer particles of the proton beam with an adjustable aperture device. Two automatic control methods for adjusting either the beam intensity or the core power have been developed. The beam intensity is adjusted automatically based on a PID controller by comparing the setting beam intensity with the measured value. On the other hand, the core power can also be controlled automatically based on the other PID controller by comparing the setting core power with the measured value. To evaluate the proposed control methods, the CiADS core model with double inputs and four outputs has been built based on the point reactor kinetics model. The simulations based on the CiADS core model have indicated that the reactor core power can be adjusted automatically by changing the aperture size. The response time in the adjustment of the core power depends mainly on the adjustment time of the aperture size.

Declaration of competing interest

The authors declare that they have no known competing financial interests or personal relationships that could have appeared to influence the work reported in this paper.

References

[1] H. Aït Abderrahim, J. Galambos, Y. Gohar, S. Henderson, G. Lawrence, T. Mcmanamy, Accelerator and Target Technology for Accelerator Driven Transmutation and Energy Production, DOE White Paper on ADS 1.1, 2010, pp. 1–23.
[2] M. Salvatores, I. Slessarev, A. Tchistiakov, G. Ritter, The potential of accelerator-driven systems for transmutation or power production using thorium or uranium fuel cycles, Nucl. Sci. Eng. 126 (1997) 333–340, https://doi.org/10.13182/NSE97-A24485.
[3] IAEA, Emerging Nuclear Energy and Transmutation Systems: Core Physics and Engineering Aspects, International Atomic Energy Agency IAEA-TECDOC-1356, August 2003.
[4] W.L. Zhan, H.S. Xu, Advanced fission energy program-ADS transmutation system, Bull. Chin. Acad. Sci. 27 (2012) 375–381.
[5] W. Zeng, T. Hui, J. Xie, T. Yu, Dynamic simulation of CIADS core power control based on the duty ratio of the proton beam, Prog. Nucl. Energy 125 (2020) 103390, https://doi.org/10.1016/j.pnucene.2020.103390.
[6] Y.M. Kim, S.P. Yun, H.S. Kim, H.J. Kwon, Beam characterization of the low-flux proton beam line at KOMAC for application to radiation effect testing, Nucl. Instrum. Methods Phys. Res. Sect. A Accel. Spectrom. Detect. Assoc. Equip. 950 (2019) 162971, https://doi.org/10.1016/j.nima.2019.162971.
[7] D.G. Sahani, S. Sharma, P. Sharma, D. Sharma, S. Hussain, Effects of Alignment of Adjustable Collimator on Dosimetric Parameters of a Telecobalt Machine, Technology in Cancer Research & Treatment 12, 2012, https://doi.org/10.7785/tcrt.2012.500308.
[8] L. Weissman, D. Berkovits, A. Arenshtam, Y. Ben-Aliz, Y. Buzaglo, O. Dudovitch, Y. Eisen, I. Eliahu, G. Feinberg, I. Fishman, I. Gavish Segev, I. Gertz, A. Grin, S. Halfon, D. Har-Even, Y. Haruvy, D. Hirschmann, T. Hirsh, Z. Horovitz, E. Zemach, SARAF Phase i linac in 2012, J. Instrum. 9 (2014), https://doi.org/10.1088/1748-0221/9/05/T05004. T05004–T05004.
[9] H. Niu, Y. Li, Y. He, B. Zhang, Z. Wang, W. Chen, C. Yuan, H. Jia, A novel adjustable aperture for beam current controlling at China-ADS low energy beam transport line, Qiangjiguang Yu Lizishu, High Power Laser and Particle Beams 32 (2020), https://doi.org/10.11884/HPLPB202032.190393.
[10] S.H. Liu, Z.J. Wang, H. Jia, Y. He, W.P. Dou, Y.S. Qin, W.L. Chen, F. Yan, Physics design of the CIADS 25MeV demo facility, Nucl. Instrum. Methods Phys. Res., Sect. A 843 (2017) 11–17, https://doi.org/10.1016/j.nima.2016.10.055.
[11] Z. Wang, Y. He, H. Jia, W. Dou, W.L. Chen, X.L. Zhang, S. Liu, C. Feng, Y. Tao, W. Wang, J. Wu, S. Zhang, H.-W. Zhao, Beam commissioning for a superconducting proton linac, Physical Review Accelerators and Beams 19 (2016), https://doi.org/10.1103/PhysRevAccelBeams.19.120101.
[12] G. Battistoni, T. Boehlen, F. Cerutti, P.W. Chin, L.S. Esposito, A. Fassò, A. Ferrari, A. Lechner, A. Empl, A. Mairani, A. Mereghetti, P.G. Ortega, J. Ranft, S. Roesler, P.R. Sala, V. Vlachoudis, G. Smirnov, Overview of the FLUKA code, Ann. Nucl. Energy 82 (2015) 10–18, https://doi.org/10.1016/j.anucene.2014.11.007.
[13] P.K. Romano, B. Forget, The OpenMC Monte Carlo particle transport code, Ann. Nucl. Energy 51 (2013) 274–281, https://doi.org/10.1016/j.anucene.2012.06.040.
[14] W.M. Schikorr, Assessments of the kinetic and dynamic transient behavior of sub-critical systems (ADS) in comparison to critical reactor systems, Nucl. Eng. Des. 210 (2001) 95–123, https://doi.org/10.1016/S0029-5493(01)00431-9.
[15] A. Cammi, L. Luzzi, A.A. Porta, M.E. Ricotti, Modelling and control strategy of the Italian LBE-XADS, Prog. Nucl. Energy 48 (2006) 578–589, https://doi.org/10.1016/j.pnucene.2006.03.006.
[16] Q. Zhang, L. Gu, T. Peng, X. Sheng, Safety analysis of CiADS sub-critical reactor fuel cladding under beam transients, Hedongli Gongcheng/Nuclear Power Engineering 39 (2018) 51–57, https://doi.org/10.13832/j.jnpe.2018.05.0051.